GEOPHYSICAL RESEARCH LETTERS, VOL. 27, NO. 17, PAGES 2693-2696, SEPTEMBER 1, 2000

Connection between Caspian Sea level variability and ENSO

K. Arpe[1], L. Bengtsson[1], G. S. Golitsyn[2], I. I. Mokhov[2], V. A. Semenov[2,1] and P. V. Sporyshev[3]

Abstract. The problem of the world greatest lake, the Caspian Sea, level changes attracts the increased attention due to its environmental consequences and unique natural characteristics. Despite the huge number of studies aimed to explain the reasons of the sea level variations the underlying mechanism has not yet been clarified. The important question is to what extent the CSL variability is linked to changes in the global climate system and to what extent it can be explained by internal natural variations in the Caspian regional hydrological system. In this study an evidence of a link between the El Niño/Southern Oscillation phenomenon and changes of the Caspian Sea level is presented. This link was also found to be dominating in numerical experiments with the ECHAM4 atmospheric general circulation model on the 20th century climate.

Introduction

Perhaps the largest regional hydrological cycle variations during the 20th century has been observed in the Caspian Sea (CS) basin [*Golitsyn*, 1995]. The CS is the world's largest closed water reservoir. Its area is now just under 400000 km^2. The catchment area of the rivers flowing into the Sea is about 3 million km^2 (close to 2% of the global land). About 80% of the river discharge into the Sea is from the Volga river which supplies on average 240 km^3. of the water annually. This amount corresponds to 60 cm of the sea level. Another 20 cm of the sea level results from the precipitation over the sea, 15 cm from other rivers. The level is balanced by evaporation and, to a small extent, by the outflow to the Bay of Kara-Bogaz-Gol at the eastern shore of the Sea where it finally evaporates. The balance is never exact and the level undergoes seasonal changes with a span of about 40 cm and experiences interannual variations.

[1]Max-Planck-Institut für Meteorologie, Hamburg, Germany

[2]Obukhov Institute of Atmospheric Physics, Moscow, Russia

[3]Voeykov Main Geophysical Observatory, St. Petersburg, Russia

Paper number 1999GL002374.
0094-8276/00/1999GL002374$05.00

Figure 1a shows interannual variations of the Caspian Sea level (CSL) for the period of instrumental observations starting in 1837 [*Golitsyn*, 1995]. Two abrupt changes of the level were observed in the 20th century. During the 1930s a fast 1.7 m drop of the CSL occurred. It was followed by a relatively slow fluctuating decrease until 1977 by another 1.2 m. A further fall seemed to be inevitable due to the increasing water consumption in the CS basin. But quite unexpectedly the CSL started to rise in 1978. From 1978 to 1995 the sea level rose by 2.5 m. The changes of the CSL are so significant that they effect all the social, economical and ecological situation in the sea region. The extraordinary rise of the CSL after 1977 is comparable in scale to its catastrophic drop in the 1930s and caused even more environmental disasters. *Rodionov* [1994] summarised possible reasons for the CSL variability. According to the recent TOPEX-POSEIDON satellite observations [*Cazenave et al.*, 1997] the CSL had been still rising until July 1995. Then it started to decrease and dropped for about 30 cm to the beginning of 1997. From then to the end of 1999 the level was relatively stable.

The first effort in applying general circulation models (GCMs) for detailed investigations of the regional CS climate was undertaken within AMIP (Atmospheric

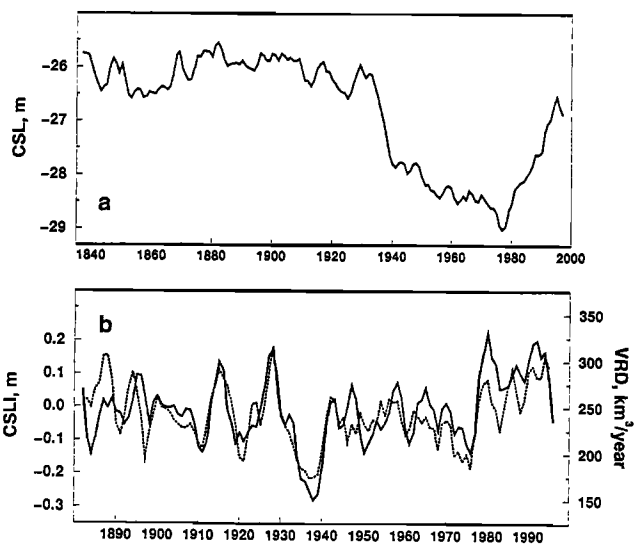

Figure 1. a) Annual mean values of the Caspian Sea level for the period of instrumental observations 1837-1997; b) annual mean values of the Caspian Sea level increments (solid line) and the VRD (3 year running means, dotted line). Note the different time axes.

Model Intercomparison Project). It was found [*Golitsyn et al.*, 1995] that most high resolution models produced similar features of interannual precipitation variability over the watershed of the Volga and Ural rivers and that simulated CSL changes were mostly determined by the river discharge variability which exceeded that of evaporation from the sea by a factor of two for the model ensemble mean.

Model simulations

In this study results of numerical experiments with the GCM ECHAM4 [*Roeckner et al.*, 1996] were used. In all simulations the atmospheric model was forced with observed sea surface temperatures, SSTs, including the sea ice boundaries [*Rayner et al.*, 1996]. Observed changes in the greenhouse gas concentration were applied as well. Four simulations were carried out for 1903-1994 and two for 1951-1994. The experiments started with different initial atmospheric conditions. The spatial resolution of the model is approximately 2.8° in latitude and longitude, so the CS is represented by 6 grid cells and 31 cells are for the catchment area of the Volga river.

The two major factors that affect the CSL are the river discharge and evaporation from the sea. A determining role of the Volga river discharge (VRD) for the interannual CSL variations is illustrated in Figure 1b where time series of the annual mean VRD [*Polonskii and Gorelits*, 1997] and annual increments of the CSL (CSLI) are presented. The correlation between CSLI and the annual river discharges is 0.82. Due to the absence of reliable SST data for the CS, the evaporation from the sea was not considered for the CS water balance computations in the model simulations. Thus in the model only the VRD taken as a difference between precipitation and evaporation averaged over the catchment area was analysed. In the following only annual means are considered which reduces the effects of river routing, which is not yet applied for the model simulations, the effect of water regulations in the Volga and the effect of snow accumulation in winter. The optimal selection of calendar months for an annual mean is discussed below.

Connections with SST anomalies

Possible relationships between the regional and global climate were estimated by a simple correlation analysis. Figure 2a shows a map of cross-correlations between annual mean SSTs (1903-1994) and observed CSLI from one year to the next one. The area of strong positive correlation covers the tropical Pacific to the east of the date line spreading further to the north and south along the continental coasts. The strongest correlation reaching 0.55 is in the central Pacific (around the dateline). Other areas of statistically significant correlations were found in the Indian Ocean and north Pacific and areas of modest correlations in the northern Atlantic. However, the correlations in the Indian Ocean and north Pacific are much lower for the shorter 1903-1975 period.

The teleconnection pattern in the north Atlantic

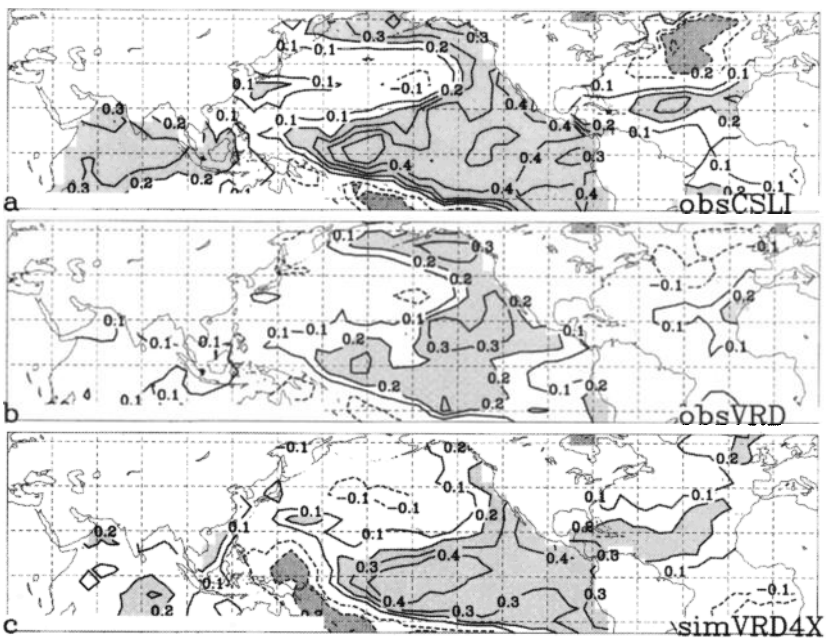

Figure 2. Maps of cross-correlations between a) CSLI (mean of following year minus mean of current year) and SSTs (1903-1994, January to December mean of current year); b) mean observed VRD (annual mean from January to December of next year) and SSTs (mean from May of current year to April next year); c) as b) but from four model experiments with VRD = precipitation – evaporation (September to August mean). Values statistically significant at the 95% level are shaded.

(negative correlation area below Greenland and positive correlation in the subtropics) will be discussed below in relation to the North Atlantic Oscillation, NAO.

Correlation maps analogous to Figure 2a were made for the observed VRD and visible evaporation (evaporation minus precipitation) from the sea taking annual mean data for 1903-1994 [*Golitsyn and Panin*, 1989]. As could be expected the VRD teleconnection map (Figure 2b) highly resembles that of CSLI though with lower values. The CS visible evaporation teleconnection map (not shown) exhibits areas of negative correlations (statistically insignificant) in the equatorial central Pacific which are similar to the pattern in Figure 2a and an area of positive correlation in the north and middle Atlantic. The opposite sign of the river discharge and visible evaporation correlation is consistent with the result obtained by *Golitsyn and Panin* [1989].

Corresponding correlation maps were made for each of the simulated VRD calculations which resulted in patterns similar to Figure 2b. The key-role of the tropical Pacific SSTs becomes apparent from a corresponding map for the simulated VRD, averaged for the four long experiments 1903-1994 (Figure 2c). This averaging reduces stochastic or "natural" variability and leaves the SST-forced signal.

The interannual SST variability in the equatorial Pacific is linked to the El Niño/Southern Oscillation phenomenon (ENSO), the dominant signal in the global climate variations with periods of 2-7 years. During a typical El Niño the SST anomalies spread from the Peru coast in spring to the central Pacific and become most intensive while during the northern Hemisphere winter. Extratropical teleconnections are known to be manifesting during the boreal winter and spring although persisting through all the El Niño event [*Rasmusson*, 1991]. Thus it would be reasonable to expect the strongest correlation with the central Pacific annual mean SSTs for which the annual averaging starts in spring-early summer and centres maximum anomalies within the averaging year.

Optimal averaging of annual means

To analyse the seasonal structure of the correlation between precipitation over the Volga Basin, VRD (both observed and modelled) and equatorial Pacific SSTs, the monthly mean data for the Niño-4 region (5°N-5°S, 150°W-160°E), located in the area of the strongest correlation with CSLI (see Figure 2), were used as an ENSO-SST index. The annual mean Niño-4 SSTs with the annual averaging starting from subsequently shifting months from January to December were correlated with annual mean series of precipitation over the Volga watershed [*Mescherskaya and Blazhevich*, 1997] and the river discharge, also with shifting annual averaging for different monthly lags.

It should be noted that annual averages (with lags) providing maximum correlation values depend on the period of analysed data and its length. In particular different 40 year periods within 1903 to 1994 were analysed. The choice of averaging period does not change the general results but gives a range of uncertainty usually not exceeding a season. Thus we refer in the following to seasons instead of months.

Both observed and modelled precipitation over the Volga basin have a maximum correlation with Niño-4 SSTs when the latter are averaged from spring to next winter. This period coincides with the typical composite El Niño year [e.g. *Torrence*, 1998]. The correlation with observed precipitation is the highest when the precipitation averaging starts from autumn. For the observed VRD the highest correlations were obtained with the same averaging of the SSTs and an averaging of the observed VRD starting in the winter of the SST averaging period.

An analysis of the seasonal mean observed precipitation versa Niño-4 SSTs lagged correlation shows that it is the autumn precipitation variability which is mostly affected by the SST variations and the river discharge is following with maximum correlations in spring.

For the seasonal mean model precipitation the correlation maximum is found in winter, i.e. simultaneous with the ENSO maximum. This difference, in particular, can be related to the differences between annual cycles for the model and observed precipitation.

Interdecadal variabilities

It is reasonable to expect that the NAO has an effect on the variability of precipitation over the Volga river basin. *Rodwell et al.* [1999] and *Latif et al.* [2000] have shown that SSTs can force the NAO on multi-annual to multi-decadal time scales. Calculating the cross-correlations in Figure 2 but applying a band pass filter for 7-25 years indeed enhances the correlation coefficients over the Atlantic (typically from 0.2 to 0.4 in Figure 2b+c) and resulting in more similar patterns over the Atlantic while the tropical Pacific is less affected. *Rodionov* [1994] discusses possible impacts of the NAO on the CSL variability. However, the prominent CSL changes in the 1930s and after 1977 have no equivalent behaviour in the NAO variability.

As the CSLIs are found to be correlated with equatorial Pacific SSTs on the interannual time-scale, the interdecadal variations of the CSL (in particular the 1930s drop and the rise in the late 1970s, Figure 1a) might as well be linked to the SST variability on the corresponding time-scale. Here some remarks should be made. Decadal equatorial Pacific SST variations were found not to be correlated with the intensity of the ENSO cycle [*Gu and Philander*, 1995]. Thus not the SST decadal variability but the ENSO frequency and amplitude variations should be analysed in order to understand decadal time scale relationships. For this purpose the Southern Oscillation Index (SOI) is more appropriate. It is defined as a normalized pressure anomaly

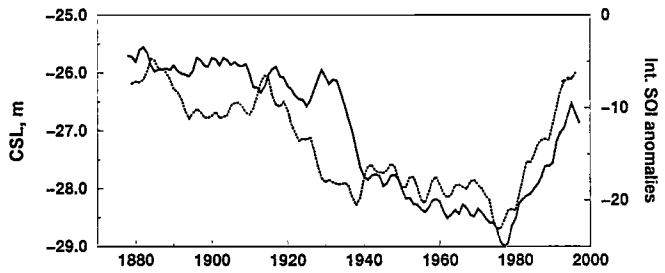

Figure 3. Time series of the Caspian Sea level (solid line) and integrated SOI anomalies averaged for December, January and February (3 year running means, dotted line).

difference between Tahiti (12°S, 150°W) and Darwin (12°S, 131°E).

The CSL and integrated values of SOI anomalies for December, January and February (the period of ENSO extremes) are presented in Figure 3 to illustrate the integrated El Niño effect. The main features of the decadal variations are similar for both time series, i.e. plateaus before 1925 and 1940-1977 and strong changes in the 1930s and after 1977. The latter rise may also be connected to the prominent increase in equatorial Pacific SSTs during that time. At the time of the river discharge drop in the 1930s no corresponding SST decrease on the decadal scale was observed, but that decade can be characterized by a long or probably the longest (1933-1938) break in El Niño occurrences in the century. There were no warm equatorial SST maxima during 1932-1939 but five subsequent cold SST minima [*Kane*, 1997]. A similar feature was also observed during 1905-1910 followed by several strong El Niño events. It is consistent with the observed river discharge variability during that time (Figure 1b).

The ENSO-CS teleconnection may be related to a change of the cyclonic activity, particularly with position and intensity of the north Atlantic and Mediterranean storm tracks, due to equator-to-pole temperature gradient change during ENSO [*Mokhov et al.*, 1995].

Acknowledgments. This study has been made possible by the technical support of the German Climate Computing Centre (DKRZ) and of the Swiss Climate Computing Centre. Computing resources were as well provided by the ECMWF special project scheme. The work was supported by the German Ministry for Education, Science Research and Technology (BMBF), EC project under the Framework IV and Russian Foundation for Basic Research (RFBR).

References

Cazenave, A., K. Bonnefond, K. Dominh, and P. Schaeffer, Caspian sea level from Topex-Poseidon altimetry: Level now falling, *Geophys. Res. Lett., 24,* 881-884, 1997.

Golitsyn, G.S., The Caspian Sea level as a problem of diagnosis and prognosis of the regional climate change, *Izv. Russ. Acad. Sci. Atmos. Oceanic Phys.*, Engl. Transl., *31,* 366-372, 1995.

Golitsyn, G. S., and G. N. Panin, The water balance and modern variations of the level of the Caspian Sea, *Soviet Meteorol. Hydrol.*, Engl. Transl., *1,* 46-52, 1989.

Golitsyn, G. S., V. P. Meleshko, A. V. Mescherskaya, I. I. Mokhov, T. P. Pavlova, V. A. Galin, and A. O. Senatorsky, GCM simulation of water balance over Caspian sea and its watershed, *Proc. First Int. AMIP Sci. Conf., USA, WMO/TD-No.732,* 113-118, 1995.

Gu, D., and S. G. H. Philander, Secular changes of annual and interannual variability in the tropics during the past century, *J. Climate 8,* 864-876, 1995.

Kane, R. P., Relationship of El Niño/Southern Oscillation and Pacific sea surface temperature with rainfall in various regions of the globe, *Mon. Weather Rev., 125,* 1792-1800, 1997.

Latif, M., K. Arpe, and E. Roeckner, Oceanic control of decadal north Atlantic sea level pressure variability in winter, *Geophys. Res. Lett., 27,* 727-730, 2000.

Mescherskaya, A. V., and V. G. Blazhevich, The drought and excessive moisture indices in a historical perspective in the principal grain-producing regions of the former Soviet Union, *J. Climate, 10,* 2670-2682, 1997.

Mokhov, I. I., V. K. Petukhov, and A. O. Senatorsky, Sensitivity of storm track activity and blockings to global climatic change: Diagnostics and modelling, *Publ. Acad. Finland, 6/95,* 438-441, 1995.

Polonskii, V. F., and O. V. Gorelits, Water runoff and its distribution in the delta of the Volga river (in Russian), *Russian Meteorol. Hydrol., 4,* 84-95, 1997.

Rasmusson, E. M., Observational aspects of ENSO cycle teleconnections, in *Teleconnections Linking Worldwide Climate Anomalies,* edited by M. H. Glantz, R. W. Katz, and N. Nicholls, pp. 309-343, Cambridge Univ. Press, Cambridge, 1991.

Rayner, N. A., E. B. Hearten, D. E. Parker, C. K. Folland, and R. B. Hacked, Version 2.2 of the global sea-ice and sea surface temperature data set, 1903-1994, *Clim. Res. Tech. Note CRTN74,* Bracknell, UK, 1996.

Rodionov, S. N., *Global and regional climate interaction: the Caspian Sea experience,* 241 pp., Kluwer Academic Publ., Dordrecht, The Netherlands, 1994.

Rodwell, M. J., D. P. Rowell, and C. K. Folland, Oceanic forcing of the wintertime North Atlantic Oscillation and European climate, *Nature. 398,* 320-323, 1999.

Roeckner, E., K. Arpe, L. Bengtsson, M. Christoph, M. Claussen, L. Dümenil, M. Esch, M. Giorgetta, U. Schlese, and Schulzweida, The atmospheric general circulation model ECHAM-4: Model description and simulation of present-day climate, *Report no. 218,* 90 pp., Max-Planck-Inst. für Meteorol., Hamburg, 1996.

Torrence, C., and P. J. Webster, The annual Cycle of persistence in the El Niño/Southern Oscillation. *Q. J. R. Meteorol. Soc., 124,* 1985-2004, 1998.

K. Arpe and L. Bengtsson, Max-Planck-Institut für Meteorologie, Bundesstr. 55, 20146 Hamburg, Germany. (e-mail: arpe@dkrz.de; bengtsson@dkrz.de)

G. S. Golitsyn, I. I. Mokhov, and V. A. Semenov, Obukhov Institute of Atmospheric Physics, 3 Pyzhevsky, 109017 Moscow, Russia. (e-mail: mokhov@omega.ifaran.ru; semenov@dkrz.de)

P. V. Sporyshev, Voeykov Main Geophysical Observatory, 7 Karbysheva, 194021 St. Petersburg, Russia. (e-mail: pvs@main.mgo.rssi.ru)

(Received July 6, 1999; accepted January 14, 2000.)